Electrical Discharge/Electrochemical Hybrid Machining Based on the Same Machine and Tool Electrode

Ryoichiro Kishi
Department of Mechanical Engineering,
Faculty of Science and Technology,
Keio University,
Hiyoshi 3-14-1,
Kohoku-ku, Yokohama 223-8522, Japan

Jiwang Yan[1]
Department of Mechanical Engineering,
Faculty of Science and Technology,
Keio University,
Hiyoshi 3-14-1,
Kohoku-ku, Yokohama 223-8522, Japan
e-mail: yan@mech.keio.ac.jp

Electrical discharge machining (EDM) causes surface defects such as resolidified layer and microcracks, and a finishing process is usually needed to remove these defects. In this paper, a hybrid process was proposed where electrochemical machining (ECM) was performed as a finishing process after EDM using the same tool electrode on the same machine. By using two kinds of disk-type rotary electrodes, rectangular grooves and grooves with convex inner structures were fabricated. Surface topography were investigated by using scanning electron microscope (SEM), energy dispersive X-ray spectrometry (EDX), and laser-probe surface profilometer. The material removal mechanism of resolidified layers was clarified. The surface roughness of the rectangular groove was improved from 3.82 μm Ra to 0.86 μm Ra after ECM. Electrode rotation was effective for flushing electrolytic products when fabricating inner structures. As there is no need for exchanging tools and machines, tool alignment error can be prevented and productivity can be improved. Therefore, the proposed EDM/ECM hybrid process contributes to rapid fabrication of microscale products with high surface integrity.
[DOI: 10.1115/1.4046039]

Keywords: ECM, EDM, hybrid machining, surface finishing, rotary tool electrode, resolidified layer, stainless steel, microstructure

1 Introduction

Electrical discharge machining (EDM) is a noncontact processing method which can machine any electrically conductive materials regardless of their hardness. EDM can also fabricate complicated microstructures [1–3]. However, EDM causes the formation of resolidified layers and microcracks on the surface due to rapid cooling effects [4,5]. When EDMed materials are used as a mold, microcracks serve as starting points of surface chippings and even mold fracturing. To remove surface defects, a finishing process is needed. Mechanical polishing is mostly used as the finishing process after EDM [6,7]. However, it is difficult to polish complicated microstructures.

Electrochemical machining (ECM) is an alternative surface finishing process [8–10]. Unlike EDMed surfaces, there is no residual stress and no affected layer in ECM [11–13]. Furthermore, ECM does not cause electrode wear [14–16]. However, most existing ECM processes are performed by changing the machine and the tool electrodes after EDM, which is time consuming and causes alignment errors. Alignment errors are critical problems in machining complicated microstructures. In recent years, hybrid EDM/ECM processes have been proposed [17–22], but there is no available literature on using disk-type rotary tool electrodes for hybrid EDM/ECM.

In this study, we propose a hybrid process of performing ECM as a finishing process after EDM. The same rotary disk-type rotary electrode was used for both ECM and EDM on the same machine to improve productivity and eliminate the alignment errors due to exchanging tools. By using a rotary disk-type rotary electrode, the surface quality and machining speed maybe improved by the flushing effect [23–25]. Moreover, it prevents from errors due to electrode wear. In this paper, voltage, tool feed rate, and tool rotation speed were varied to investigate the machining performance. The capability of high precision machining of complicated grooves without tool alignment errors was demonstrated.

2 Experimental Method

A copper disk (diameter 51 mm and thickness 2 mm) and another copper disk with a 500 μm wide groove in the circumference were used as electrodes. The nongrooved disk was used to fabricate a rectangular groove, and the grooved disk was used to fabricate a groove with a convex inner structure. The workpiece was stainless steel SUS304 fabricated by rolling process and cut into blocks by wire-EDM. The size of the grooves to machine was 0.3 mm in depth, 2 mm in width, and 3 mm in length. The tank for EDM oil and ECM electrolyte was mounted on the stage of EDM machine (Mitsubishi, Japan, EA8PV). The jig for holding the workpiece was fixed on the tank (see Fig. 1).

At first, EDM was performed by filling the tank with EDM oil. After EDM, the oil was drained and the tank was refilled with ECM electrolyte. Then, ECM was performed as the finishing process by using the same electrode and machine used for EDM. A stabilized DC power supply (Kikusui, Japan, PAS160-2) was used for the ECM. The hybrid process is schematically shown in Fig. 2. The machining conditions for EDM and ECM are shown in Tables 1 and 2, respectively. Based on the results of machining

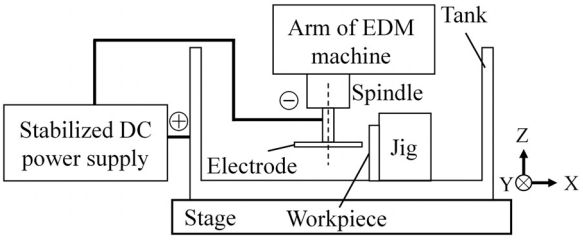

Fig. 1 Schematic of the experimental setup

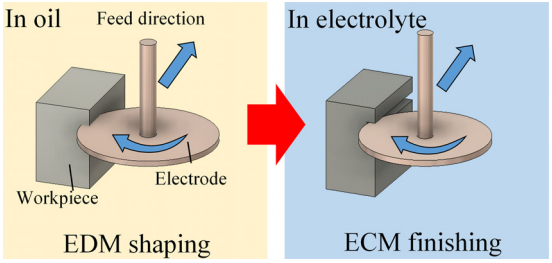

Fig. 2 EDM/ECM hybrid machining process

[1]Corresponding author.

Contributed by the Manufacturing Engineering Division of ASME for publication in the Journal of Micro- and Nano-Manufacturing. Manuscript received October 31, 2019; final manuscript received December 17, 2019; published online February 13, 2020. Assoc. Editor: Lawrence Kulinsky.

Table 1 Machining conditions in EDM

Electrode's polarity	Positive
Current (A)	4
Pulse on time (μs)	246
Duty ratio	50%
Rotation speed (rpm)	500
Feed rate (mm/min)	0.3

Table 2 Machining conditions in ECM

Voltage: V (V)	6, 8
Rotation speed: ω (rpm)	0, 500, 1000, 2000
Feed rate: f (mm/min)	0 (for 3 min), 1, 3
Solution	2 wt % $NaNO_3$
Current type	DC

Table 3 Machining conditions in ECM for grooves with convex inner structures

Exp. no.	V (V)	f (mm/min)	ω (rpm)
1	6	1	0
2	6	1	500
3	6	1	1000
4	8	1	0
5	8	1	500
6	8	3	1000

rectangular grooves, conditions were selected for fabricating grooves with convex inner structures (see Table 3). Tool path in ECM was the same as that in EDM. Thus, the ECM gap was also the same as that in EDM (about 65 μm).

Scanning electron microscope (SEM: FEI, Hillsboro, OR, Inspect S50) was used to observe the machined surface. Energy dispersive X-ray spectrometry (EDX: HITACHI, Japan, TM3030) was used to analyze the components of the resolidified layer. A laser-probe surface profilometer (Mitaka, Japan, MP-3) was used for measuring the surface roughness and the cross-sectional profiles. The surface roughness was measured five times along the same direction of tool feed path.

3 Results and Discussion

3.1 Removal Mechanism of Resolidified Layer. Scanning electron microscope images of the EDMed and ECMed surfaces are shown in Fig. 3. As shown in Fig. 3(*a*), the EDMed surface is covered by a resolidified layer. There are craters and microcracks on the surface. After ECM, residual pieces of the resolidified layer are observed on the surface (Fig. 3(*b*)). The resolidified layer has been broken into small pieces along the microcracks. The size of the divided resolidified layer is about 10∼100 μm. The resolidified layer is completely removed at higher voltages and lower rotation speeds (Figs. 3(*c*) and 3(*d*)). Finally, the waviness of the surface was also improved, as shown in Fig. 3(*d*).

The debris in the ECM electrolyte was collected by a paper filter and observed by SEM. Figure 4 shows the SEM image and EDX analysis of the debris. The size of debris is comparable to the size of the divided resolidified layer of EDM. In EDX analysis, Fe and Cr were detected in the debris as shown in Fig. 4. Since Fe and Cr are the main components of stainless steel, the debris in

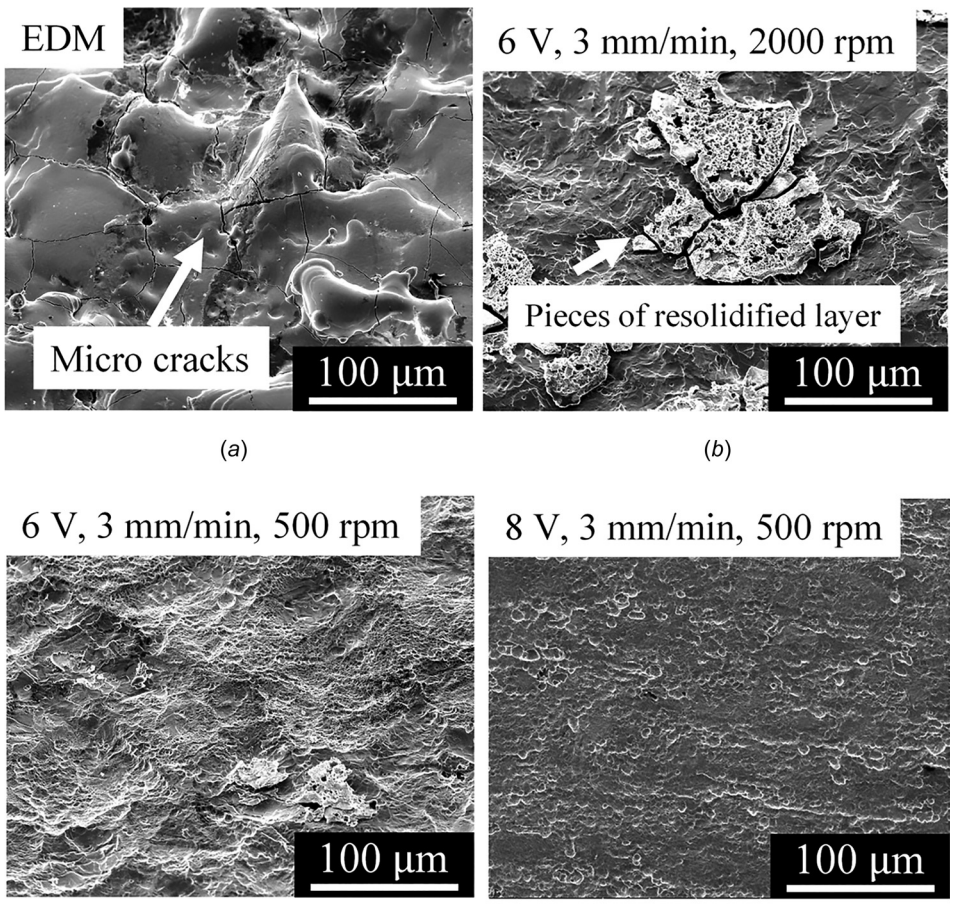

Fig. 3 Machined surfaces by (*a*) EDM and (*b*)–(*d*) ECM

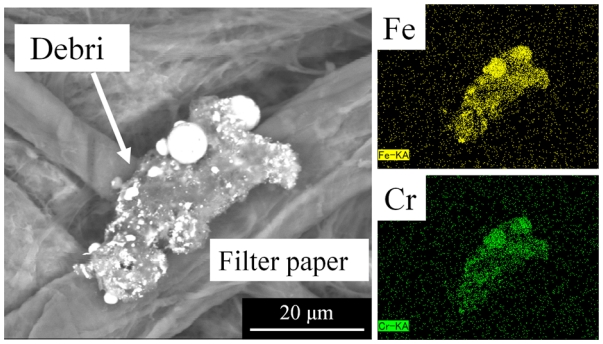

Fig. 4 SEM image and EDX results of debris

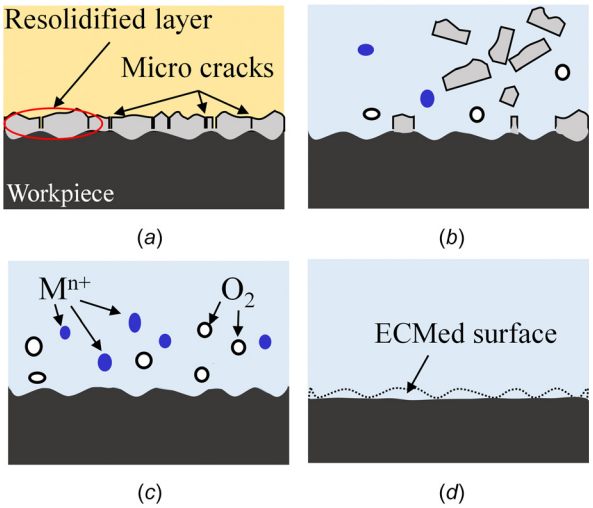

Fig. 5 Removal mechanism of resolidified layer: (*a*) after EDM, (*b*) early stage of ECM, (*c*) middle stage of ECM, and (*d*) end stage of ECM

Fig. 4 should be a part of the resolidified layer of EDM, rather than the electrolytic products.

According to the observation results, the possible material removal mechanism is shown in Fig. 5. At first, the resolidified layer breaks into small pieces along microcracks (Fig. 5(*a*)). The pieces of the resolidified layer are peeled by ECM due to the tensile residual stress and bubbles (Fig. 5(*b*)). The residual stress also helps to expand the microcracks. ECM-induced bubbles remove the pieces of the resolidified layer from the unaffected bulk workpiece. Subsequently, ECM continues on the waved surface of the bulk workpiece and generates electrolytic products such as M^{n+} and O_2 (Fig. 5(*c*)). Finally, the waved surface of the bulk becomes smooth (Fig. 5(*d*)).

3.2 Effect of Tool Electrode Rotation. In order to examine the effect of rotation of the tool electrode, ECM without tool rotation and ECM with tool rotation were carried out. Figure 6 shows the SEM images of a surface obtained by ECM without tool rotation. It is clear that ECM was not performed uniformly; smooth regions and rough regions are observed on the surface.

Figure 7 shows a comparison of the surface ECMed without tool rotation and with tool rotation. To eliminate possible tool feed effect, no tool feed was used and the machining time was 3 min for both conditions. In the center region of surface, the gap between the workpiece and the electrode is minimum. Without tool rotation, the resolidified layer remained on the center of surface though there is no resolidified layer in the outer region (Fig. 7(*a*)). In contrast, the resolidified layer was completely removed from the surface by introducing the tool rotation (Fig. 7(*b*)).

Figure 8 shows schematically the effect of tool electrode rotation. In the case of no tool rotation, the electrolytic products remain in the gap between the electrode and the workpiece. In addition, the ECM-induced bubbles remain in the gap which inhibits the electric current. Thus, ECM was carried out locally. On the other hand, tool rotation induces a strong flushing effect which makes electrolytic products flow out of the gap easily. Therefore, the electrical current in the gap is stable and continuous.

3.3 Effect of Voltage. The results of ECMed surface roughness at $V = 6$, 8 V are shown in Figs. 9 and 10, respectively. It is a general trend that surface roughness is improved by using a higher voltage, lower tool feed rate, and lower tool rotation speed. The lowest surface roughness was 0.86 μm Ra obtained when $V = 8$ V, $f = 1$ mm/min, and $\omega = 0$ rpm. By using a high rotation speed, the number of microbubbles increased. While microbubbles induce a flushing effect, they also act as an insulator restricting current to flow, as shown in Fig. 8. Accordingly, generation of a lot of

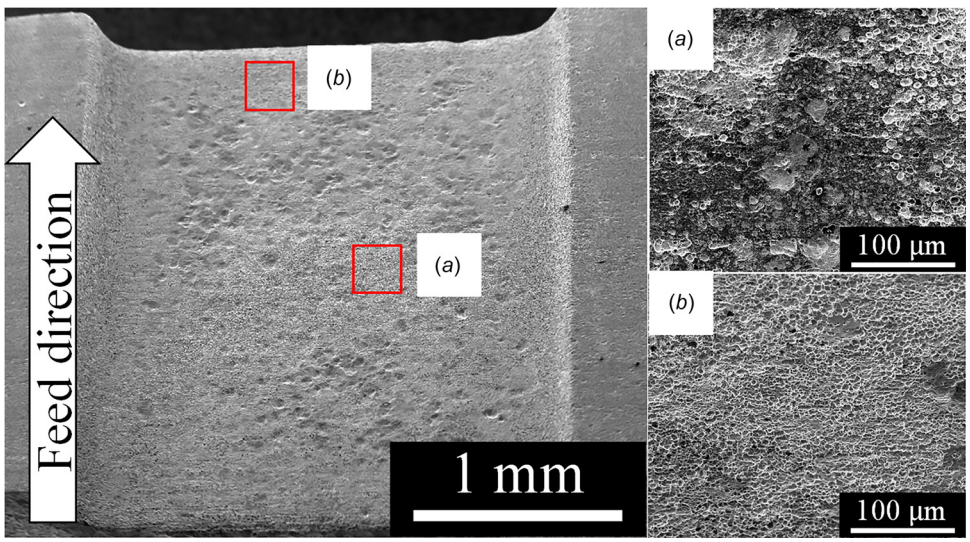

Fig. 6 Nonuniformly ECMed surface at $V = 6$ V, $f = 3$ mm/min: (*a*) smooth region and (*b*) rough region

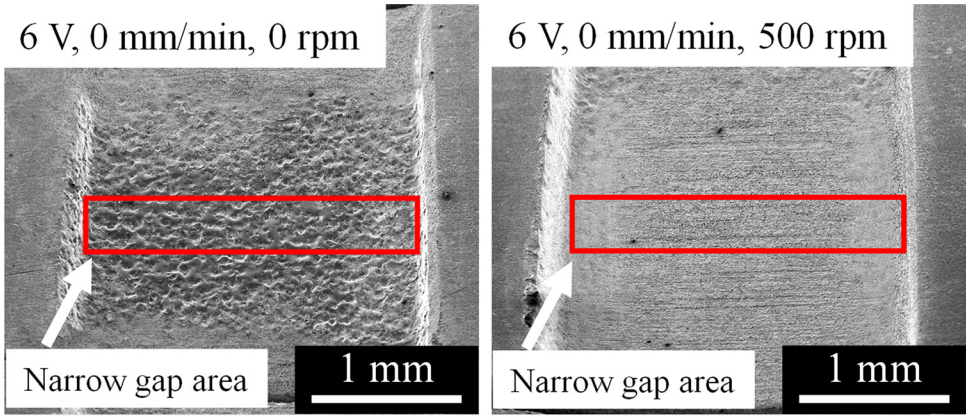

(*a*) (*b*)

Fig. 7 ECMed surface without tool feed for 3 min: (*a*) without tool rotation and (*b*) with tool rotation

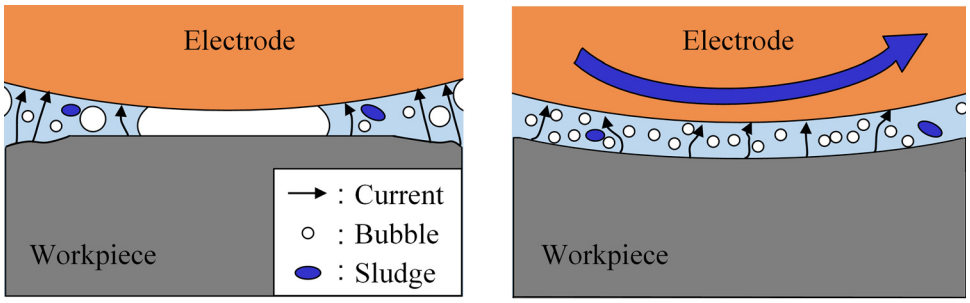

(*a*) (*b*)

Fig. 8 Schematic of tool rotation effect: (*a*) without tool rotation and (*b*) with tool rotation

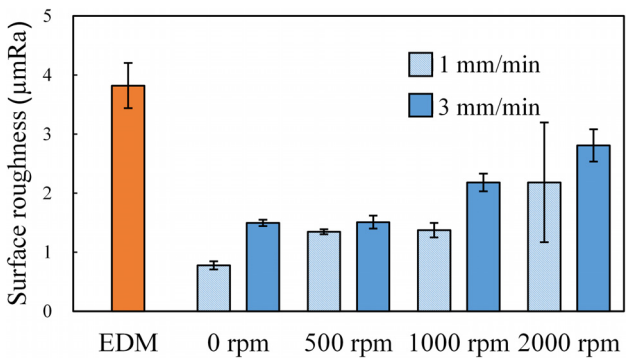

Fig. 9 Surface roughness of ECM at 6 V

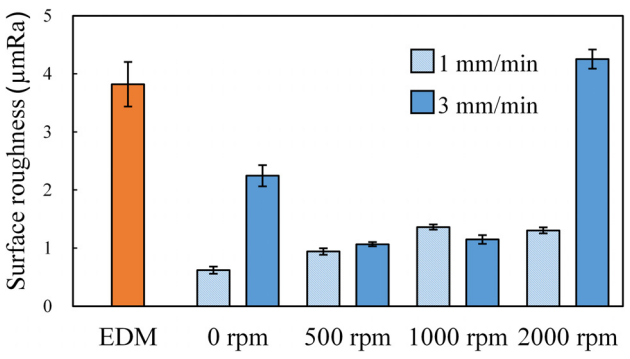

Fig. 10 Surface roughness of ECM at 8 V

microbubbles decreases processing efficiency [26–28]. Also, the resolidified layer remained due to the decrease of processing efficiency, and the remaining resolidified layer results in the rough surface. When $V = 8$ V, $f = 3$ mm/min, and $\omega = 2000$ rpm, the ECMed surface was rougher than the EDMed surface. This might be because a few pieces of resolidified layer were peeled off by the strong flow of fluid, leaving some craters on the surface, as can be seen in Fig. 11. It was these craters that increased surface roughness. Tool feed rate is related to ECM processing time. A lower feed rate leads to a longer processing time, but produces smoother surfaces. When the voltage is increased, the material removal rate increases [29,30]. Thus, ECM processing speed is increased by using a higher voltage. In summary, the conditions of higher voltage, lower feed rate, and lower tool rotation speed are advantageous in terms of not only removing the resolidified layer but also smoothing the wavy bulk surface.

3.4 Effect of Tool Electrode Shape. Figure 12 shows the SEM images of ECMed surfaces of such grooves at $V = 8$ V with/without tool rotation. The resolidified layer has been completely removed for both conditions, and the wavy surface of the bulk unaffected by EDM was smoothened by ECM. However, in the case of no tool rotation, the edge of the convex inner structures became round (Fig. 12(*a*)). The complicated shape of the electrode-workpiece gap inhibited the flushing of the electrolytic from the gap. Thus, using tool rotation is suitable for fabricating grooves with inner structures in terms of the flushing effect.

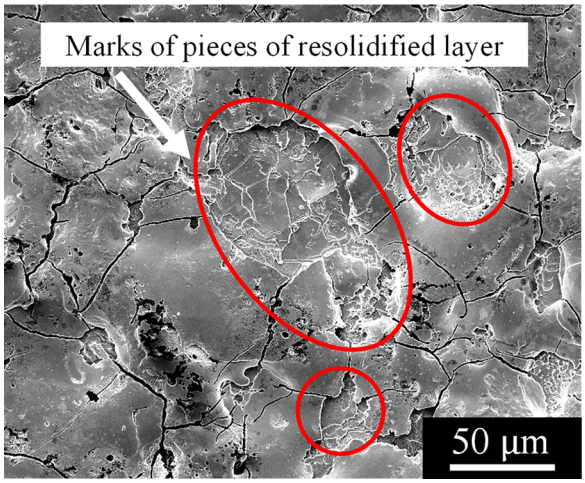

Fig. 11 ECMed surface ($V = 8$ V, $f = 3$ mm/min, and $\omega = 2000$ rpm)

The cross-sectional profiles of the EDMed and ECMed groove surfaces at $V = 8$ V are shown in Fig. 13. The corner of the groove with inner structures became rounded at $f = 1$ mm/min and $\omega = 0$ rpm. However, the corners became distinctly shaper at $f = 3$ mm/min and $\omega = 1000$ rpm. Therefore, in order to prevent corner rounding, using a higher feed rate and a higher rotation speed is effective for machining complicated grooves with inner structures. In addition, in this research, a DC power supply was used, thus machining localization was significant. To improve the form accuracy, using a high-frequency pulse power supply might be a solution because a pulse current can decrease the effect of machining localization [31–33]. This will be one of our future tasks.

Figure 14 shows the surface roughness of grooves with inner structures obtained at various ECM conditions. The lowest surface roughness was 1.05 μm Ra, and then $V = 8$ V, $f = 1$ mm/min, and $\omega = 500$ rpm were obtained. On the other hand, the highest surface roughness 2.88 μm Ra was produced at $V = 8$ V, $f = 1$ mm/min, and $\omega = 0$ rpm. From these results, it can be concluded that the disk-type rotary electrode is effective to improve surface roughness for generating complicated grooves with convex inner structures.

3.5 Electrode Wear. To confirm the electrode wear, we measured the cross-sectional profiles of EDMed grooves after the first and the fourth grooving cycles, and the result was shown in Fig. 15. The difference in the average depth of the two grooves was 2.4 μm, thus the electrode wear for one machining cycle was estimated to be 0.8 μm. Although this electrode wear is very small, it will affect the form accuracy of the machined grooves and should be compensated in high-precision product fabrication.

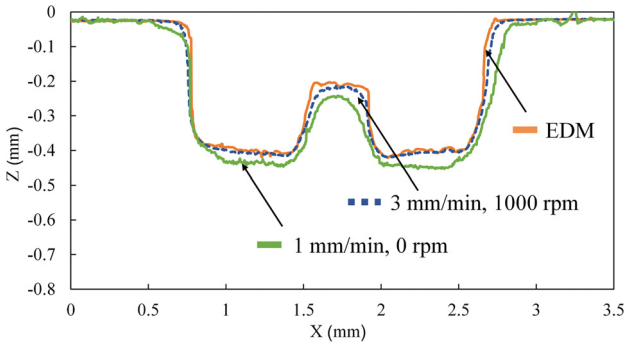

Fig. 13 Cross-sectional profiles of grooves

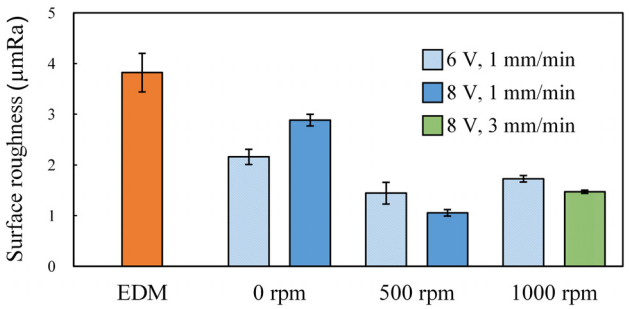

Fig. 14 Surface roughness for various conditions

4 Conclusions

A hybrid process was proposed where ECM was performed as a finishing process of EDM without changing the tool electrode and machine, and its fundamental characteristics were investigated. Two kinds of grooves including those having convex inner structures were fabricated by using disk-type rotary tool electrodes. The main findings include the following:

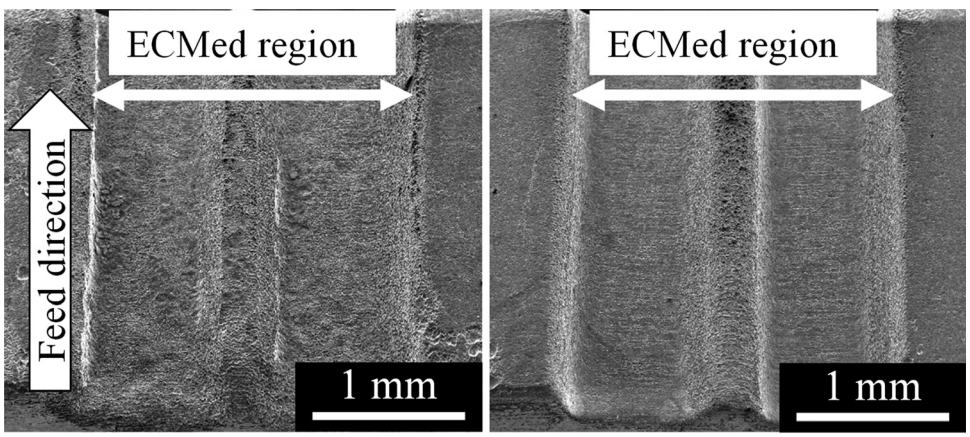

(*a*) (*b*)

Fig. 12 ECMed surfaces of grooves with convex inner structures: (*a*) without tool rotation and (*b*) with tool rotation

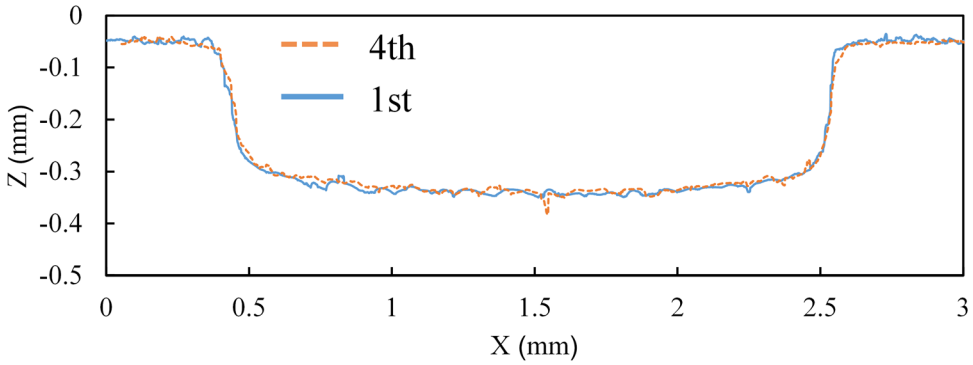

Fig. 15 Cross-sectional profiles of EDMed grooves

(1) The resolidified layer formed in EDM was disassembled along the microcracks in ECM, and finally, removed as small pieces, leaving a smooth surface.
(2) The surface roughness of rectangle grooves was improved from 3.82 μm Ra to 0.86 μm Ra at $V = 8$ V and $f = 1$ mm/min without tool rotation.
(3) The rotation of the disk-type electrode was effective to flush electrolytic products and acquire high surface integrity on complicated grooves with convex inner structures.
(4) Using a higher feed rate and a higher rotation speed was effective to reduce the edge rounding effect and improve the form accuracy.

References

[1] Wang, D., Zhao, W. S., Gu, L., and Kang, X. M., 2011, "A Study on Micro-Hole Machining of Polycrystalline Diamond by Micro-Electrical Discharge Machining," J. Mater. Process. Technol., **211**(1), pp. 3–11.
[2] Xu, B., Wu, X. Y., Ma, J., Liang, X., Lei, J. G., Wu, B., Ruan, S. C., and Wang, Z. L., 2016, "Micro-Electrical Discharge Machining of 3D Micro-Molds From $Pd_{40}Cu_{30}P_{20}Ni_{10}$ Metallic Glass by Using Laminated 3D Micro-Electrodes," J. Micromech. Microeng., **26**(3), pp. 1–10.
[3] Shih, H. R., and Shu, K. M., 2008, "A Study of Electrical Discharge Grinding Using a Rotary Disk Electrode," Int. J. Adv. Manuf. Technol., **38**(1–2), pp. 59–67.
[4] Peças, P., and Henriques, E., 2008, "Electrical Discharge Machining Using Simple and Powder-Mixed Dielectric: The Effect of the Electrode Area in the Surface Roughness and Topography," J. Mater. Process. Technol., **200**(1–3), pp. 250–258.
[5] Ekmekci, B., 2007, "Residual Stresses and White Layer in Electric Discharge Machining (EDM)," Appl. Surf. Sci., **253**(23), pp. 9234–9240.
[6] Hsue, A. W. J., and Chang, Y. F., 2016, "Toward Synchronous Hybrid Micro-EDM Grinding of Micro-Holes Using Helical Taper Tools Formed by Ni-Co/Diamond Co-Deposition," J. Mater. Process. Technol., **234**, pp. 368–382.
[7] Peças, P., and Henriques, E., 2003, "Influence of Silicon Powder-Mixed Dielectric on Conventional Electrical Discharge Machining," Int. J. Mach. Tools Manuf., **43**(14), pp. 1465–1471.
[8] Lappin, D., Mohammadi, A. R., and Takahata, K., 2012, "An Experimental Study of Electrochemical Polishing for Micro-Electro-Discharge-Machined Stainless-Steel Stents," J. Mater. Sci. Mater. Med., **23**(2), pp. 349–356.
[9] Ma, N., Xu, W., Wang, X., and Tao, B., 2010, "Pulse Electrochemical Finishing: Modeling and Experiment," J. Mater. Process. Technol., **210**(6–7), pp. 852–857.
[10] Ramasawmy, H., and Blunt, L., 2007, "Investigation of the Effect of Electrochemical Polishing on EDM Surfaces," Int. J. Adv. Manuf. Technol., **31**(11–12), pp. 1135–1147.
[11] Kurita, T., Chikamori, K., Kubota, S., and Hattori, M., 2006, "A Study of Three-Dimensional Shape Machining With an ECμM System," Mach. Tools Manuf., **46**, pp. 1311–1318.
[12] Spieser, A., and Ivanov, A., 2015, "Design of a Pulse Power Supply Unit for Micro-ECM," Int. J. Adv. Manuf. Technol., **78**(1–4), pp. 537–547.
[13] Spieser, A., and Ivanov, A., 2015, "Design of an Electrochemical Micromachining Machine," Int. J. Adv. Manuf. Technol., **78**(5–8), pp. 737–752.
[14] Yu, N., Fang, X., Meng, L., Zeng, Y., and Zhu, D., 2018, "Electrochemical Micromachining of Titanium Microstructures in an NaCl–Ethylene Glycol Electrolyte," J. Appl. Electrochem., **48**(3), pp. 263–273.
[15] Cle, O. L. A., 2007, "A Study of the Characteristics for Electrochemical Micromachining With Ultrashort Voltage Pulses," Int. J. Adv. Manuf. Technol., **31**(7–8), pp. 762–769.
[16] Xu, Z., Chen, X., Zhou, Z., Qin, P., and Zhu, D., 2016, "Electrochemical Machining of High-Temperature Titanium Alloy Ti60," Procedia CIRP, **42**, pp. 125–130.
[17] Wu, X., Li, S., Jia, Z., Xin, B., and Yin, X., 2019, "Using WECM to Remove the Recast Layer and Reduce the Surface Roughness of WEDM Surface," J. Mater. Process. Technol., **268**, pp. 140–148.
[18] Zeng, Z., Wang, Y., Wang, Z., Shan, D., and He, X., 2012, "A Study of Micro-EDM and Micro-ECM Combined Milling for 3D Metallic Micro-Structures," Precis. Eng., **36**(3), pp. 500–509.
[19] Nguyen, M. D., Rahman, M., and Wong, Y. S., 2013, "Transitions of Micro-EDM/SEDCM/Micro-ECM Milling in Low-Resistivity Deionized Water," Int. J. Mach. Tools Manuf., **69**, pp. 48–56.
[20] Kurita, T., and Hattori, M., 2006, "A Study of EDM and ECM/ECM-Lapping Complex Machining Technology," Int. J. Mach. Tools. Manuf., **46**(14), pp. 1804–1810.
[21] Cheng, G., Jun, Q., and Dominiek, R., 2016, "Finishing of Micro-EDMed Surface Based on Scanning Micro Electrochemical Flow Cell," Procedia CIRP, **42**, pp. 834–841.
[22] Wu, X., Li, S., Zhao, W., Tang, L., and Li, Z., 2019, "Experiment Investigation of Using Wire Electrochemical Machining in Deionized Water to Reduce the Wire Electrical Discharge Machining Surface Roughness," Int. J. Adv. Manuf. Technol., **102**(1–4), pp. 343–353.
[23] Singh, S., and Pandey, A., 2013, "Some Studies Into Electrical Discharge Machining of Numonic75 Super Alloy Using Rotary Copper Disk Electrode," J. Mater. Eng. Perform., **22**(5), pp. 1290–1303.
[24] Yan, B. H., Wang, C. C., Liu, W. D., and Huang, F. Y., 2000, "Machining Characteristics of Al_2O_3/6061Al Composite Using Rotary EDM With a Disk-like Electrode," Int. J. Adv. Manuf. Technol., **16**(5), pp. 322–333.
[25] Koshy, P., Jain, V. K., and Lal, G. K., 1993, "Experimental Investigations Into Electrical Discharge Machining With a Rotating Disk Electrode," Precis. Eng., **15**(1), pp. 6–15.
[26] Yan, Z., Zhengyang, X., Jun, X., and Di, Z., 2016, "Effect of Tube-Electrode Inner Diameter on Electrochemical Discharge Machining of Nickel-Based Superalloy," Chin. J. Aeronaut., **29**(4), pp. 1103–1110.
[27] Shimasaki, T., and Kunieda, M., 2016, "Study on Influences of Bubbles on ECM Gap Phenomena Using Transparent Electrode," CIRP Ann.-Manuf. Technol., **65**(1), pp. 225–228.
[28] Zhang, X., Li, H., Yin, Z., and Ren, K., 2019, "Influence of Bubbles on Micro-Dimples Prepared by Electrochemical Micromachining," J. Appl. Electrochem., **49**(10), pp. 963–978.
[29] Bhattacharyya, B., and Munda, J., 2003, "Experimental Investigation on the Influence of Electrochemical Machining Parameters on Machining Rate and Accuracy in Micromachining Domain," Int. J. Mach. Tools Manuf., **43**(13), pp. 1301–1310.
[30] Bhattacharyya, B., Malapati, M., and Munda, J., 2005, "Experimental Study on Electrochemical Micromachining," J. Mater. Process. Technol., **169**(3), pp. 485–492.
[31] Schuster, R., Kirchner, V., Allongue, P., and Ertl, G., 2000, "Electrochemical Micromachining," Science, **289**(5476), pp. 98–101.
[32] Bhattacharyya, B., Doloi, B., and Sridhar, P. S., 2001, "Electrochemical Micro-Machining: New Possibilities for Micro-Manufacturing," J. Mater. Process. Technol., **113**(1–3), pp. 301–305.
[33] Kozak, J., Rajurkar, K. P., and Makkar, Y., 2004, "Study of Pulse Electrochemical Micromachining," J. Manuf. Processes, **6**(1), pp. 7–14.